Pure & Appl.Chem., Vol.53, pp.2167-2179.
Printed in Great Britain.

0033-4545/81/112167-13$02.00/0
Pergamon Press Ltd

INTERACTIONS IN MIXED COLLOIDAL SYSTEMS (HETEROCOAGULATION, ADHESION, MICROFLOTATION)

Egon Matijević

Institute of Colloid and Surface Science and Department of Chemistry, Clarkson College of Technology, Potsdam, New York 13676, USA

Abstract - The topic deals with interactions in three different types of systems: (1) particle/particle, (2) particle/plane, and (3) particle/bubble. Essentially, the same fundamental theory applies in all cases.
(1) Mixed systems can be obtained by coprecipitation of different solids from homogeneous solutions, by precipitation of one (or more) solids in the presence of a preformed sol, or by mixing different preformed dispersions. In the last case the properties of the mixed system will greatly depend on the relative sizes of the dispersed matter. When unlike particles are of comparable size either heterocoagulation or selective coagulation can be expected. If the system consists of particles greatly different in size, adsorption of small particles on the large ones may take place, in addition to other phenomena. Examples of above cases are given and the results, where possible, interpreted in terms of the double layer forces based on the Poisson-Boltzmann equation in its two-dimensional form.
(2) Particle adhesion can be treated as a special case of particle/particle interactions by letting the radius of one particle extend to infinity. Carefully executed studies of the kinetics of adsorption of well defined metal oxides on steel and their detachment from such surfaces as a function of various parameters are described and interpreted.
(3) Particle/bubble interactions are discussed in relationship to removal of finely dispersed matter by microflotation. Organic and inorganic suspended colloidal particles can be efficiently separated as long as they are flocculated and the bubble size is rather small ($\sim$50 μm). It is shown that this process is much more rapid than settling or filtration.

INTRODUCTION

Interactions in mixtures of colloids are important for two reasons: (1) they represent challenging problems from experimental and theoretical points of view, and (2) they are of interest in a variety of applications, including corrosion, detergency, flotation, filtration, water purification, paint formulation, to mention just a few. The topic is sufficiently broad to cover a variety of phenomena, which may occasionally appear unrelated, yet the same underlying principles apply. This presentation deals with interactions in systems consisting of

I. Mixtures of unlike particles (heterocoagulation),

II. Particles in contact with a plane surface (adhesion), and

III. Particle/bubble mixtures (microflotation).

The work considers chemical and physical aspects of these interactions and shows that in properly defined systems the double layer theory based on the two-dimensional Poisson-Boltzmann (P.-B.) equation explains well the observed phenomena.

I. MIXTURES OF UNLIKE PARTICLES

Most work in colloid dispersions has treated single systems; i.e. sols consisting of one kind of particles. In contrast, the majority of dispersions that occur in nature or are used in various applications contain particles which differ in composition, size, shape, and other properties.

As is commonly the case in the study of colloidal systems, mixed dispersions can be treated from the chemical or physical points of view or both. In many cases it is impossible to develop a proper physical model since the chemistry of the system may be either too complicated or even unknown.

Mixed colloidal dispersions can be, in principle, obtained by:

1. Precipitation from homogeneous solutions,
2. Precipitation of one component in dispersions which already contain one or more kinds of particles, and
3. Mixing dispersions of different particles.

1. Precipitation from homogeneous solutions

Precipitation of mixed solids in a given system is essentially a problem of carrying out properly designed chemical reactions. For illustration, phenomena observed when solutions of $Al(NO_3)_3$ at low pH and of Na_2SiO_3 at high pH are mixed at constant temperature will be

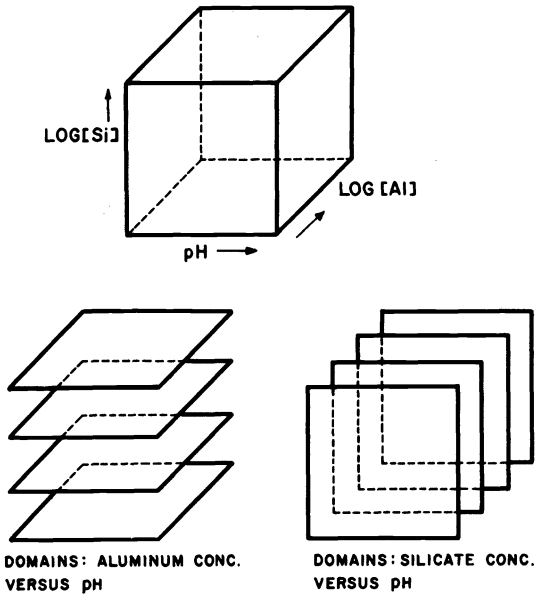

Fig. 1.

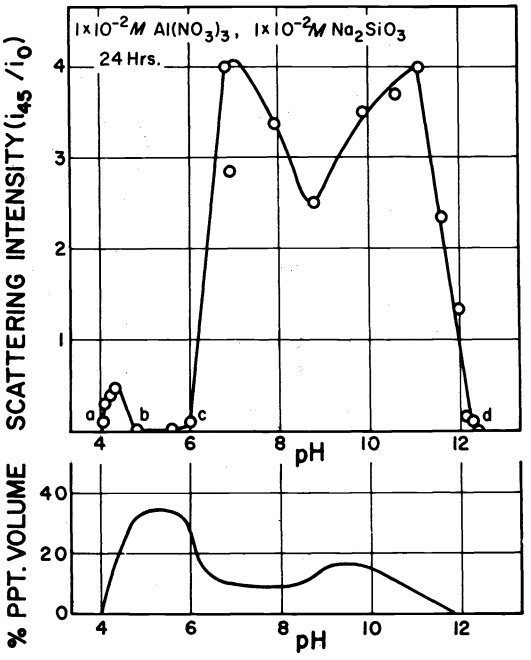

Fig. 2.

Fig. 1. The three-dimensional matrix showing the reaction variables. Horizontal cross-sections correspond to the effect of aluminum concentration and pH for various silicate concentrations. Vertical sections allow silicate and pH effects to be represented at fixed aluminum salt concentrations. (Ref. 1).

Fig. 2. Relative scattering intensities and precipitate volumes as a function of pH of systems obtained 24 hours after mixing aluminum nitrate and sodium silicate solutions. Final concentrations: 1 x 10^{-2} *M* $Al(NO_3)_3$ and 1 x 10^{-2} *M* Na_2SiO_3. Extrapolation of scattering intensities to zero (a-d) gives the respective boundaries for stability/precipitation domains (see Fig. 3).(Ref. 1).

discussed (Ref. 1). Addition of an acid to the former or a base to the latter allows a study of the solid phase formation over a broad pH range. Three parameters can be varied, i.e. concentrations of the two precipitating reactants and pH. Experimentally, it is convenient to keep one of these components constant, while systematically altering the other two. This procedure permits the construction of the boundaries designating conditions for phase formation and/or dispersion stability, which then gives the three-dimensional precipitation domain as illustrated in Fig. 1.

Optical methods, such as measurements of turbidities or light scattering intensities, are most convenient for the detection of changes that take place on mixing the reacting solutions. Other techniques must be used for better characterization of the resulting products. Figure 2 gives as an example the changes in turbidity and in the precipitate volume in a series of systems in which the concentrations of $Al(NO_3)_3$ and Na_2SiO_3 were kept constant,

whereas pH was varied in small increments. Several regions, indicating systems of different properties, can be distinguished. A series of cross-sections as shown in Fig. 2 yield two-dimensional precipitation domains as exemplified in Fig. 3. No solid phase forms in regions A and B, stable dispersions are obtained under conditions designated by IV and VI, and coagulated systems result under III and VIII. Obviously, sodium silicate exercises no effect at concentrations $<10^{-3}M$. A section of the domain 3b is reproduced on an enlarged scale with additional information in Fig. 4. In the upper part are given lines of equal relative turbidity and in the lower part are shown lines of equal electrokinetic mobilities. It is quite clear, that unstable precipitates are associated with low electrokinetic potentials. Regions VI and IV correspond to positively and negatively charged alumosilicates, respectively. Additional such domains yield the three-dimensional diagram (Fig. 1) which allows a prediction of the natures of the alumosilicate products precipitated under a given set of conditions.

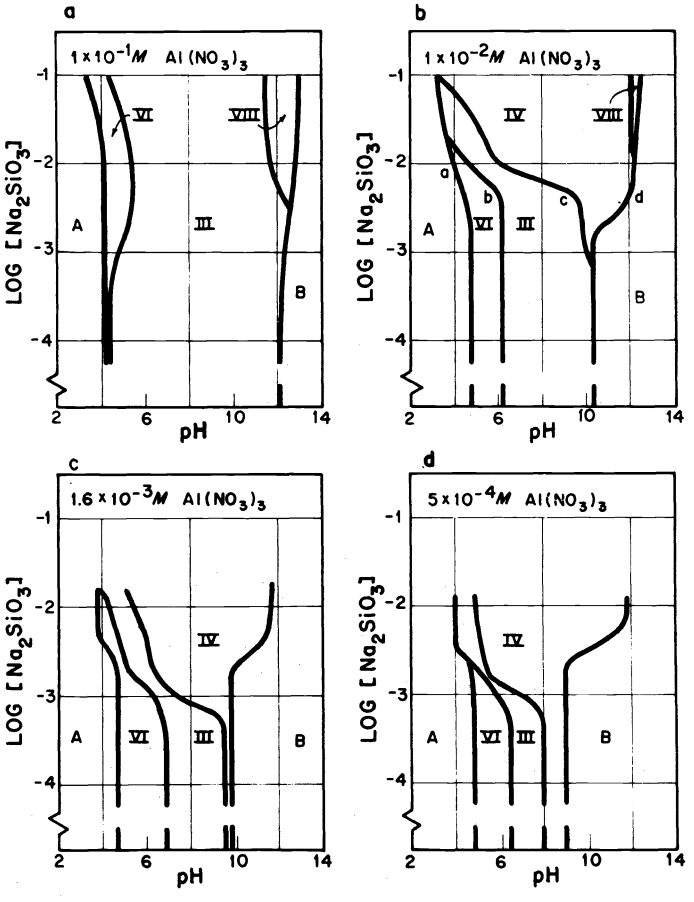

Fig. 3. Precipitation/stability domains for systems containing (a) 1×10^{-1} M, (b) 1×10^{-2} M, (c) 1.6×10^{-3} M, and (d) 5×10^{-4} M $Al(NO_3)_3$ and varying concentrations of sodium silicate as a function of pH, 24 hours after mixing the reacting components. Regions A and B consist of true ionic solutions and the Roman numerals denote precipitation regions of different stabilities as described in text. Precipitates in region VIII formed slowly over 24 hours.(Ref. 1).

2. Precipitation of one component in an existing colloidal dispersion

As an example will serve again an "alumosilicate" system with the difference that as starting material is used an aqueous dispersion of Ludox silica to which is added a solution of an aluminum salt and then the pH is adjusted (Ref. 2). Figure 5 (right) delineates various boundaries as a function of pH and the concentration of the aluminum salt. Each region (designated by Roman numerals) represents a system of different composition and properties. Thus, in I and VII silica sol is stable; in II it is coagulated, and in VI restabilized (due to charge reversal) by complex aluminum cations. In region III, which is known as the "sweep zone" in water chemistry, particles of silica heterocoagulate with positively charged

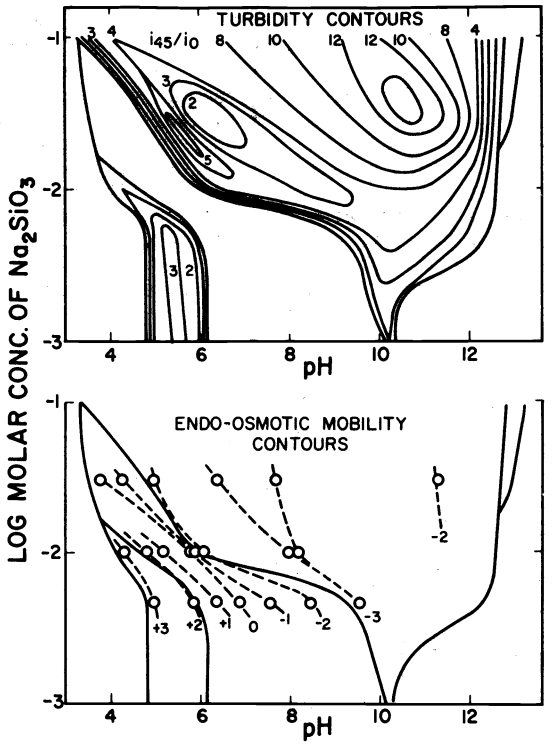

Fig. 4. The enlarged upper portion of the precipitation/stability domain of Fig. 3b indicating the systems of the same scattering intensities (above) and the same endo-osmotic mobilities (below) within the various precipitation regions.(Ref. 1).

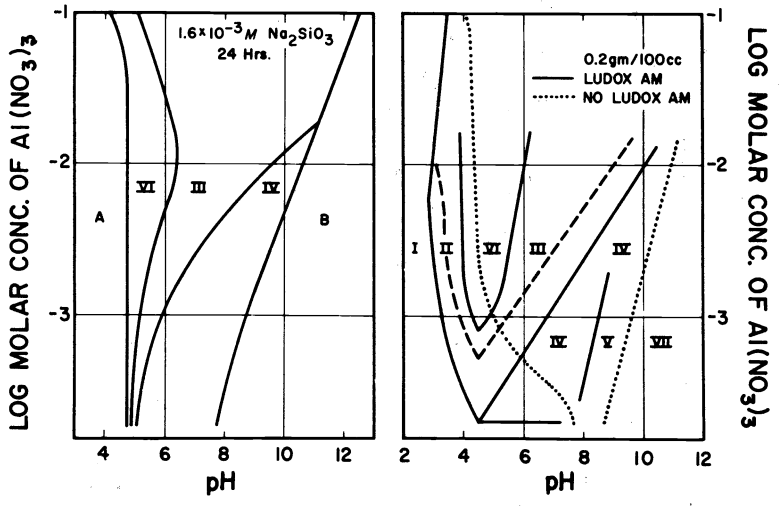

Fig. 5. Right. Aluminum nitrate-pH domain for the Ludox AM sol. The solid lines designate regions of various degrees of sol stability, 24 hours after mixing the reaction components. I, stable sols; II, sols coagulated by soluble aluminum species; III, coprecipitated and flocculated silica and aluminum hydroxide; IV and V, stable, highly negatively charged coprecipitates of silica and aluminum hydroxide; VI, stable sols of reversed charge. Region within the dotted lines indicates the precipitation domain of aluminum hydroxide in the absence of silica. Dashed line designates the points of zero charge of the precipitates.
Left. Precipitation/stability domain for systems containing $1.6 \times 10^{-3} M$ Na_2SiO_3 and various concentrations of $Al(NO_3)_3$ as a function of pH. Regions *A* and *B* consist of ionic solutions and the Roman numerals denote precipitation regions of different stabilities as described above.(Ref. 1 & 2).

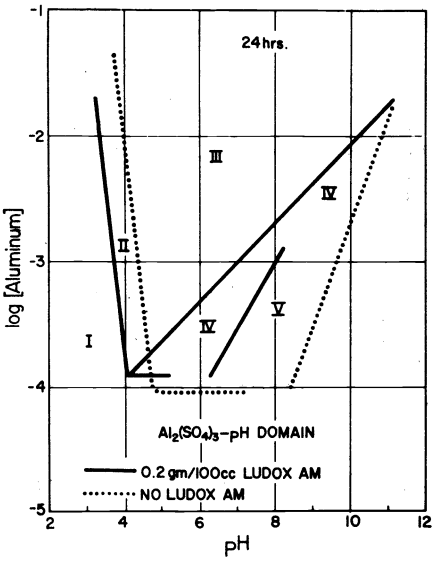

Fig. 6.

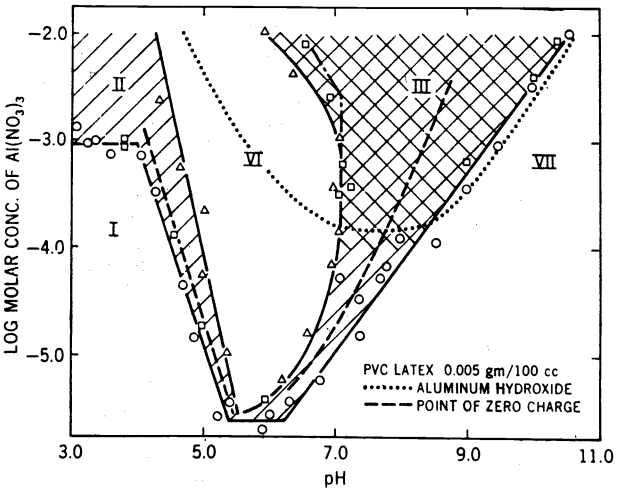

Fig. 7.

Fig. 6. Aluminum sulfate - pH domain for the Ludox AM sol. The solid lines designate regions of various degrees of sol stability 24 hours after the mixing of the components (Ref. 2). For explanation of different regions see Fig. 5.

Fig. 7. Stability domain for PVC latex in the presence of $Al(NO_3)_3$ as a function of pH determined 4 h (□) and 24 h (○,△) after mixing the reacting components: (...) precipitation boundary of aluminum hydroxide; (---) points of zero charge; (-·-·) stability boundary of aluminum hydroxide. The hatched areas represent unstable sols. In regions I and VII, the latex is stable and negatively charged in the presence of solute aluminum species. In region II, the latex is coagulated by solute aluminum species and in region III latex and aluminum hydroxyde coprecipitate. Region IV represents restabilized latex due to charge reversal by hydrolyzed aluminum ions or precipitated aluminum hydroxide. (Ref. 5).

precipitated aluminum hydroxide. It is noteworthy that at low pH values silica sols are stable even at high $Al(NO_3)_3$ concentrations. Under these conditions the particles are uncharged which would appear to contradict the expected behavior of colloidal dispersions. However, the stability properties of silica can be explained by considering hydration of the particles and their ion exchange properties (Ref. 3 & 4).

Left-hand side of Fig. 5 describes the precipitation/stability diagram obtained by mixing solutions of $Al(NO_3)_3$ and Na_2SiO_3 as described earlier. The main features of this domain were essentially the same as for the Ludox sol, which indicates the dominant role which aluminum chemistry plays in determining the colloidal properties of the investigated systems.

When aluminum nitrate is substituted by aluminum sulfate, the main boundaries remain similar, except that region VI is missing (Ref. 2). The latter is due to coagulation effect of the sulfate ion on silica sols of reversed (positive) charge (Fig. 6).

It is well known that Ludox silica is a typical hydrophilic colloid. One would expect corresponding stability diagrams for hydrophobic colloids to be somewhat different as indeed shown in the example of the PVC latex in the presence of $Al(NO_3)_3$ (Ref. 5). In regions II, III, VI, and VII (Fig. 7) latex behaves analogously to silica. However, at low pH (region I) Al^{3+} ion destabilizes the dispersion above the critical coagulation concentration characteristic of counterions of 3+ charge. It should be noted that the different boundaries can be quantitatively interpreted by considering equilibria involving various aluminum species in solution (Ref. 6 & 7).

3. Dispersions of unlike particles

Until recently most studies in heterocoagulation dealt with polymer colloids (various latexes) because of their perfectly spherical particles of exceedingly narrow size distributions. In recent years, however, a number of "monodispersed" metal (hydrous) oxide and sulfide systems have been prepared consisting of particles of various compositions and shapes, including spheres (Ref. 8 & 9). The advantage of the latter dispersions is in the ease with which the particle potential can be systematically changed simply by altering the pH. Mixtures of such sols with latexes allow the study of interactions in systems of two kinds of unlike particles whose potentials can be varied readily.

In principle two cases can be distinguished in mixed dispersions. In the first case, the unlike solids greatly differ in size; consequently, the number of the very much smaller particles must be considerably greater than of the large particles in order to detect any significant effects. In such systems one may expect the adsorption of small particles on the large ones, heterocoagulation, or selective coagulation. In the second case, in which the particles are of comparable sizes and number concentrations, only heterocoagulation or selective coagulation can take place.

In any mixture of colloids the charge of the solids plays an important role: the particles of opposite charge attract each other, whereas the particles of like charge repel each other. However, the same statement does not hold for potentials: unlike particles of the same sign of potential may undergo attraction and of opposite sign of potential repulsion. As a consequence the behavior of mixed dispersions is much more difficult to interpret and predict.

In the absence of specific chemical reactions between solids and solutes, dispersions containing unlike solids can be treated quantitatively by employing a properly formulated theory of the electrical double layer. For any theoretical interpretation of the data the systems must consist of reasonably uniform spherical particles of known surface potentials, Hamaker constants, and number concentrations, whereby the ionic strength also plays an essential role.

The problem of interactions of unequal spheres was dealt with by Hogg, Healy, and Fuerstenau (HHF) (Ref. 10) who developed an approximate expression for the double layer energy utilizing the procedure which Derjaguin applied to equal spheres (Ref. 11 & 12). Most of the comparisons of the experimental data with theoretical expectations were made using the HHF model and it was invariably found that the calculated double layer energies were considerably larger than the experimentally established values (Ref. 13-18).

More recently the double layer interactions of unlike spheres were examined in terms of the two-dimensional Poisson-Boltzmann equation (to be designated as the BMRF model) and it was found that the derived expression (Ref.19) much better described the observed data (Ref. 15-18).

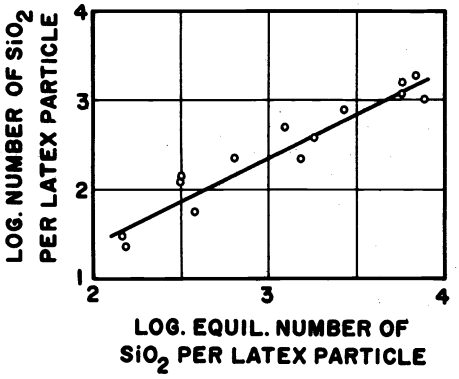

Fig. 8. Deposition (adsorption isotherm) of Ludox HS silica on PVC latex in 0.001 mol dm^{-3} 1-1 electrolyte at pH 3.2. (Ref. 20).

A. Unlike particles of considerably different sizes

The first example deals with a system consisting of relatively large polyvinyl chloride (PVC) latex (modal diameter 510 nm) and very small Ludox silica particles (modal diameter 27 nm) (Ref. 20). Figure 8 shows the adsorption isotherm for this system which confirms that under certain conditions silica particles are taken up by latex although both solids are negatively charged. The number of adsorbed silica particles as determined experimentally and calculated from theory agreed to within ± 10%.

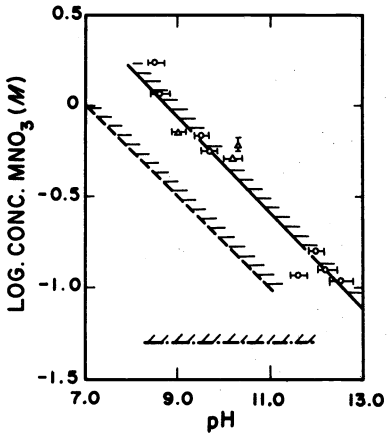

Fig. 9.

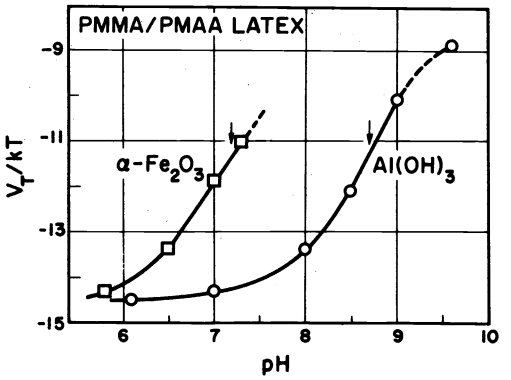

Fig. 10.

Fig. 9. Critical coagulation concentration of $NaNO_3$ (○) and KNO_3 (△) as a function of pH for 2 g dm^{-3} Ludox HS silica (---), 0.05 g dm^{-3} PVC latex (-·-·-) and a binary mixture of these sols (—) obtained 24 h after preparing the systems. Unstable dispersions are on the shaded side. Error bars denote the experimental reproducibility for the binary mixtures. (Ref. 20).

Fig. 10. Experimental values of V_T/kT at 25°C and KNO_3 1 x 10^{-2} M as a function of pH for adsorption of PMMA/PMAA latex (particle diameter d = 80 nm) on spherical aluminum hydroxide particles (d = 500 nm), ○; and on spherical hematite particles (d = 550 nm), □. (Ref. 18).

Latex modified by adsorption of silica behaved quite differently in the presence of electrolytes than the pure system. Figure 9 demonstrates that the binary mixture is more stable with respect to the addition of an 1-1 electrolyte than either of the single sols. In the presence of Ca^{2+} under certain conditions (low concentration of Ca^{2+}) selective coagulation was established; i.e., silica was coagulated while latex remained dispersed. At sufficiently high additions of $Ca(NO_3)_2$ heterocoagulation took place.

It was also shown that small latex particles [poly(methyl methacrylate co-methacrylic acid), PMMA/PMAA] can adsorb on much larger aluminum hydroxide or hematite spheres (Ref. 18). From data obtained at different temperatures the total interaction energies, V_T, between the latex and either of the two metal (hydr)oxides were established. Figure 10 gives this information as a function of pH, in which the arrows indicate the isoelectric points for the two adsorbents. At these pH values the double layer effect is negligible so that the entire measured energy corresponds to the van der Waals contribution (V_A). The latter is independent of pH making it possible to evaluate the double layer energies (V_E) at pH's different than the i.e.p. and to compare these with the theoretically estimated quantities. Table 1 gives the corresponding results showing an excellent agreement between the experimental data and the values calculated from the BMRF expression. In contrast, the HHF equation yields much too high energies at all reasonable separations.

TABLE 1. Calculated interaction energies for the PMMA/PMAA latex + hydrated aluminum oxide system at different particle separations (Ref. 18). (Experimentally determined value $V_E \approx -3.2\ kT$)

h_o/nm	HHF V_E/kT	BMRF V_E/kT	V_A/kT
5	-21	-0.5	-0.9
2	-71	-1.8	-2.9
1	-124	-3.2	-6.2
0.6	-166	-4.3	-10.8
0.5	-183	-4.7	-13.1

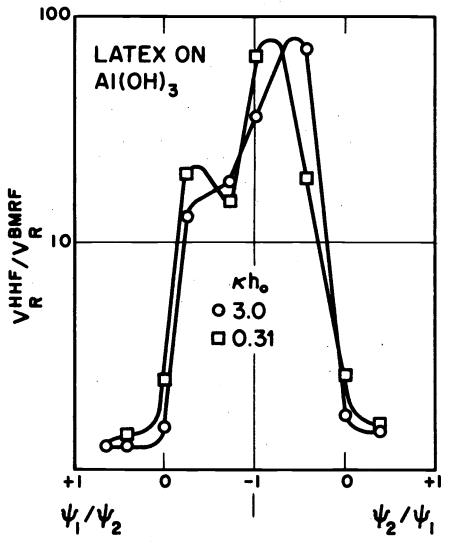

Fig. 11.

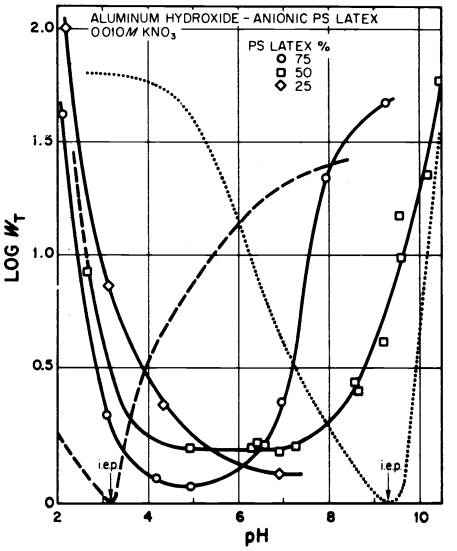

Fig. 12.

Fig. 11. The ratio of calculated double layer energies using the HHF (V_E^{HHF}) and BMRF (V_E^{BMRF}) expressions for the system consisting of PMMA/PMAA latex and aluminum hydroxide (Ref. 18) as a function of the ratio of potentials (ψ_1/ψ_2 and ψ_2/ψ_1) at κh_0 values 3.0 (○) and 0.31 (□).

Fig. 12. Overall stability ratio, W_T, for the mixture of anionic PS latex (particle 1) and aluminum hydroxide (particle 2) as a function of pH at a constant ionic strength (0.010 *M* KNO_3). Particle number fraction of anionic PS latex: 1.0 (---), 0.75 (○), 0.50 (□), 0.25 (◇), 0 (·····). Total particle number concentration: 1.12 x 10^8 per cm^3 (Ref. 15).

In order to see if the discrepancies as calculated using the BMRF and HHF models are more general than for the illustrated case, extensive analysis was carried out for the same system but over a broad range of potentials on the two kinds of particles. Figure 11 shows that HHF consistently gives higher double layer energies, although the ratios of V_E^{HHF}/V_E^{BMRF} vary over a broad range of values. Similar (and even larger) discrepancies were obtained with other calculated cases (Ref. 21).

B. Unlike particles of comparable size

Stability phenomena in dispersions of unlike particles of comparable size were also investigated using mixtures of latex and metal oxide particles. In Fig. 12 the overall stability ratio (log W_T) is plotted as a function of pH for a system of spherical aluminum hydroxide particles (diameter: 0.57 μm) and an anionic polystyrene latex (diameter 0.38 μm). A comparison of certain experimental and calculated values of W_T and W_{12} for this and other studied systems is offered in Table 2. Again, the BMRF model gives much more reasonable stability constants than those based on the HHF expression (Ref. 15).

II. PARTICLE ADHESION

In principle particle adhesion on plane surfaces can be treated as a system of two unlike particles taking the radius of one to be infinitely large. Of equal interest are problems related to particle adsorption as to particle removal. Extensive studies of particle adhesion and removal phenomena have been made using the packed column technique. Specifically, the interactions of spherical colloidal hematite and chromium hydroxide particles with steel have been carried out as a function of pH and various electrolyte additives (Ref. 16 & 22). When steel beads used in the packed column are 100-200 times larger than the suspended particles, the filtration effect is negligible and any particle removal by the column is due to adhesion.

TABLE 2. A comparison of the experimental and calculated values of W_T and W_{12} at pH 3.0 using BMRF model and HHF model (Ref. 15).

System	Particle no. ratio	W_T Exptl.	W_T BMRF	HHF
Anionic PS latex + cationic PS latex	25:75	4	24	1.6×10^4
	50:50	2	18	4.1×10^3
Aluminum hydroxide + anionic PS latex	25:75	3	240	1.8×10^3
	50:50	5	350	1.6×10^4
		W_{12}		
Anionic PS latex + cationic PS latex		3	9	2×10^8

Figure 13 shows that the uptake of hematite by steel depends strongly on pH; the maximum effect is observed when the difference of potentials of opposite sign on the particles and on the substrate is the largest (Ref. 16).

Particle removal phenomena are much more involved. In order to affect the desorption of adhered particles, it is necessary to alter the conditions in the rinsing solution. The experiments were carried out as to avoid any but diffusion forces. The most important parameters affecting particle detachment are the pH and ionic strength. Careful kinetic studies

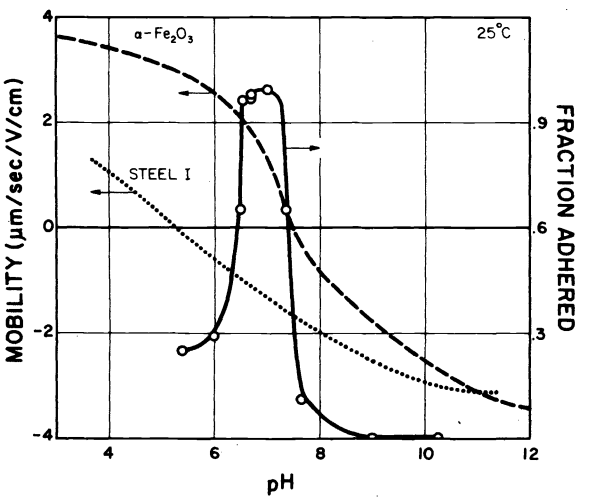

Fig. 13.

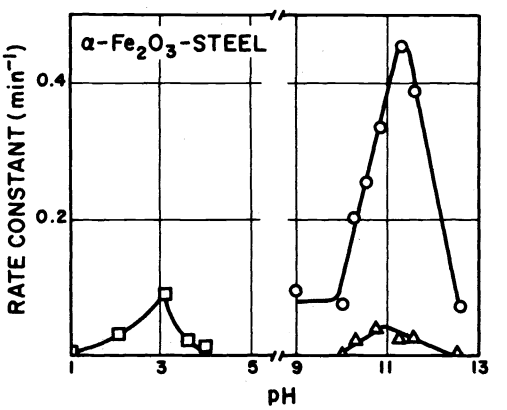

Fig. 14.

Fig. 13. Fraction of spherical α-Fe_2O_3 particles (d = 0.17 μm) deposited on steel as a function of pH at 25°C. In each case a 50-cm^3 α-Fe_2O_3 sol of $\sim 10^8$ particles/cm^3 was passed through the bed at a flow velocity of $\sim$ 0.03 cm sec^{-1}. Electrophoretic mobilities of hematite and of steel particles are shown by dashed and dotted lines, respectively. (Ref. 16).

Fig. 14. Rate constants for the removal of spherical α-Fe_2O_3 particles (d = 0.19 μm) from steel as a function of pH.

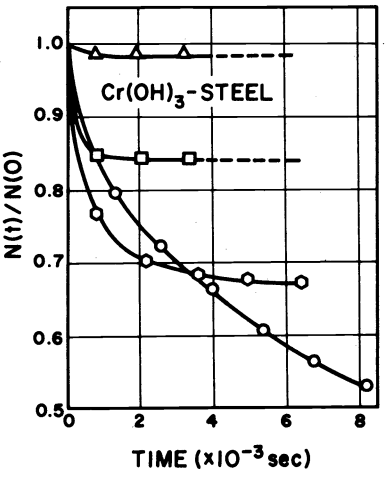

Fig. 15.

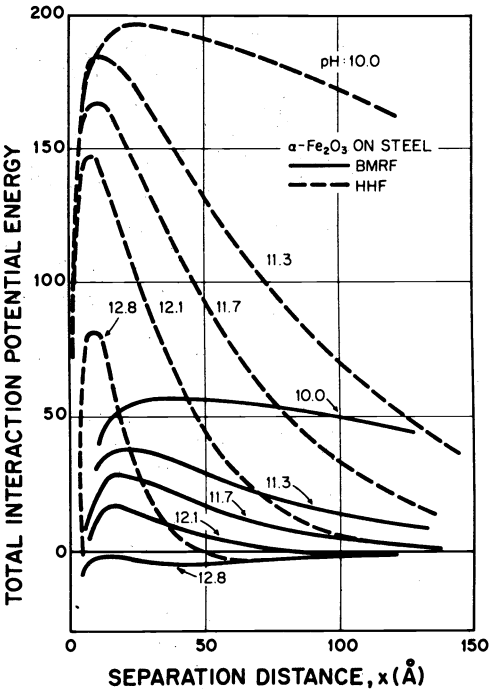

Fig. 16.

Fig. 15. Effect of different concentrations of $Ca(NO_3)_2$ on desorption of spherical chromium hydroxide particles (d = 0.28 μm) from steel. Adsorption pH 5.0, desorption pH 11.7. Concentration of $Ca(NO_3)_2$ in mol dm^{-3}: △, 1×10^{-3}; □, 1×10^{-4}; ⬡, 1×10^{-5}; ○, zero (Ref. 22).

Fig. 16. Calculated total potential energy V_T/kT as a function of distance of separation for the system spherical α-Fe_2O_3 particles (d = 0.17 μm) and steel beads using the BMRF model (full lines) and the HHF model (dashed lines) (Ref. 16).

(Ref. 23) have shown that a fraction of adsorbed particles cannot be removed regardless of pH of the wash solution. Particles that can be removed, do so at two rather different rates over a narrow pH range (Fig. 14). It was established that the topography of the steel surface was responsible for the observed effects. Particles embedded in crevices cannot be removed by diffusion alone even under most favorable conditions of pH and ionic strength. The most readily desorbed particles are those which adhere to the flat surface and require the lowest energy of activation. The slow detachment is characteristic of particles under conditions between the two extreme cases.

The particle removal can be greatly affected by addition of electrolytes. Figure 15 shows that the presence of calcium ions can strongly inhibit desorption of chromium hydroxide from steel.

The examples offered here indicate that the phenomena of particle adhesion and removal are governed by the properties of the electrical double layers on the substrate and on the suspended solids. Again, in the absence of chemical bonds, which is the case in the chosen systems, the theory of the interactions of unlike particles should apply.

Figure 16 gives the total interaction energies for hematite on steel as a function of separation between the particle and the surface (Ref. 16). The dashed lines are calculated using the HHF expression for the double layer contribution to the total energy, whereas solid lines are based on the BMRF model. Obviously, the energy barriers as evaluated from HHF equation are much too high to allow for the removal of adhered particles by diffusion only. In contrast, calculations using the two-dimensional Poisson-Boltzmann equation (BMRF) nicely agree with the observed phenomena. At pH values for optimal removal the energy barriers are low corresponding to even smaller energies of activation; thus, the kinetic energy suffices for particles to escape. At high pH values the particles are attracted

over all separations and cannot leave the surface. Finally, at pH 10 the energy barrier is reasonably high and it extends far into the solution allowing no particle detachment. Similar results have been observed with several different studied systems (Ref. 16 & 17). These examples show that particle adhesion phenomena can be explained if adequate theoretical treatment of the double layer is applied.

III. PARTICLE-BUBBLE MIXTURES (MICROFLOTATION)

Systems consisting of fine bubbles and particles represent interesting and useful mixed dispersions; they permit the study of multicomponent systems with a negative overall Hamaker constant. Unfortunately, no reliable data of bubble potentials in aqueous media in the absence of surfactants have been reported as yet. As a consequence it is not possible to evaluate the necessary interaction parameters, although any interpretation would have to take into consideration special properties of bubble surfaces.

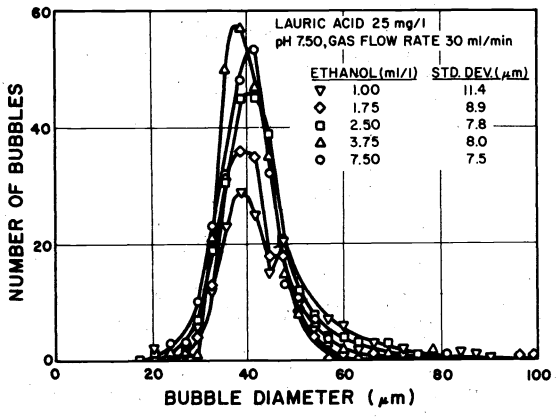

Fig. 17. Bubble size distributions as a function of various ethanol concentrations in solutions containing lauric acid (25 mg l^{-1}) at pH 7.5 and for a gas flow rate of 30 ml min^{-1} Ethanol concentrations: ▽1.0, ◇1.75, □2.5, △3.75, and ○7.5 ml l^{-1}. (Ref. 24).

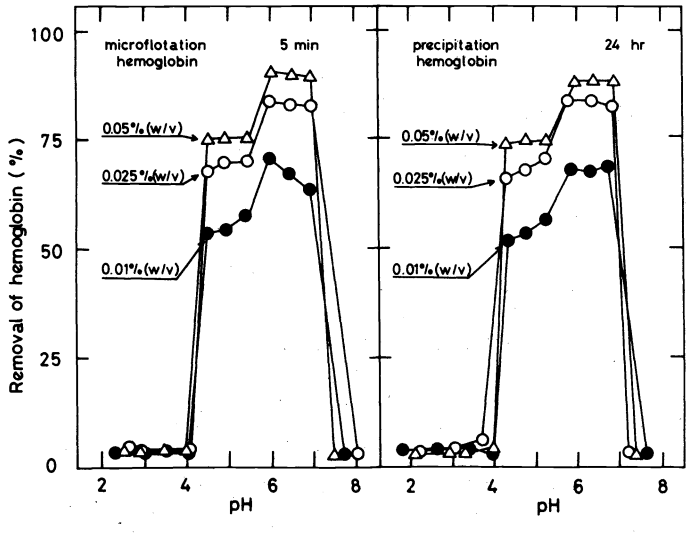

Fig. 18. Plots of percentage removal of hemoglobin (isoelectric point 6.7) after 5 min of microflotation (left) or 24 hr of precipitation (right) as a function of pH at three protein concentrations [0.05% (△); 0.025% (○); 0.01% (w/v) (●)] in the absence of added electrolyte. (Ref. 25).

In this review the application of microbubbles to the removal of colloids from solutions by flotation will be described. It was shown that finely dispersed solids of any composition can be rapidly separated by foaming as long as the bubbles are sufficiently small (diameter ∿50 μm) and the particles to be removed are in flocculated state. The latter can be accomplished by heterocoagulation with a metal hydroxide precipitated *in situ* over an appropriate pH range. Small additions of a collector (lauric acid) are also needed.

It is interesting that microbubbles of narrow size distribution can be obtained if a gas is forced through a fine frit into water containing a small amount (<1%) of lower alcohols (Fig. 17). No satisfactory explanation of this effect has been found as yet (Ref. 24).

Figure 18 illustrates microflotation data for hemoglobin in the absence of an added electrolyte (Ref. 25). The protein can be removed quantitatively from the aqueous solution over the pH range in the vicinity of the i.e.p. In the same figure is also shown that hemoglobin flocculates and settles over the same pH range, but that the latter separation process takes considerably longer times than microflotation.

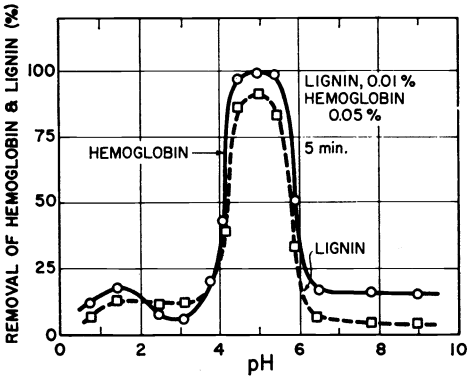

Fig. 19

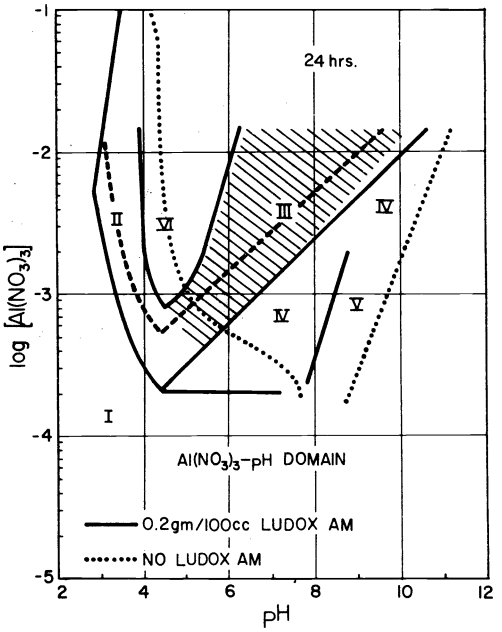

Fig. 20.

Fig. 19. Percentage removal of lignin (dashed line) and of hemoglobin (solid line) after 5 min microflotation as a function of pH. Kraft lignin, 0.01 wt%; hemoglobin, 0.05 wt%; lauric acid, 1.25×10^{-4} *M*; ethanol, 2.5 ml/liter. (Ref. 26).

Fig. 20. Aluminum nitrate - pH stability domain for the Ludox AM sol: (——) regions of various degrees of sol stability 24 hr after mixing of the components. For explanations of these regions see Fig. 5. Hatched area designates 50% or greater removal of silica after 5 min of microflotation. (Ref. 32).

In the second example (Fig.19) is demonstrated that the mixture of a protein and lignin can be efficiently removed by flotation with microbubbles. (Ref. 26). Other organic suspended matter, including bacteria, latex, humic acid, etc. (Ref. 27-30) could be separated by the same procedure, particularly when aluminum hydroxide was precipitated prior to bubble passage through the suspension.

Different inorganic dispersions (silica, metal hydroxides) were also successfully and rapidly removed by microflotation (Ref. 31 & 32). The stability diagram of silica in the presence of $Al(NO_3)_3$ is reproduced in Fig. 20 which indicates the optimal conditions (shaded area) of silica separation (Ref. 32). Obviously, successful microflotation coincided with region III (the sweep-zone). Such data were helpful in establishing the mechanism of the process involved in the removal of colloid particles by bubbles.

Acknowledgement - This work was supported by the NSF grants ENG 78-27577 and CHE 80-13684. The author is greatly indebted to his many collaborators and specifically to Dr. A. Bleier; Mr. R. Brace, Dr. F. K. Hansen, Dr. N. Kallay, Dr. M. Koishi, Dr. R. Kuo, Dr. F. T. Mangravite, Jr., and Dr. H. Sasaki on whose work is based the major part of this presentation. Many useful discussions with Professor E. Barouch (Clarkson College) are gratefully acknowledged.

REFERENCES

1. R. Brace and E. Matijević, Colloid Polymer Sci. 255, 153 (1977).
2. E. Matijević, F. J. Mangravite, Jr. and E. A. Cassell, J. Colloid Interface Sci. 35, 560 (1971).
3. L. H. Allen and E. Matijevic, J. Colloid Interface Sci. 31, 287 (1969).
4. L. H. Allen and E. Matijević, J. Colloid Interface Sci. 33, 420 (1970).
5. E. Matijević and A. Bleier, Croat. Chem. Acta 50, 93 (1977).
6. E. Matijević, K. G. Mathai, R. H. Ottewill and M. Kerker, J. Phys. Chem. 65, 826 (1961).
7. E. Matijevic, G. E. Janauer and M. Kerker, J. Colloid Sci. 19, 333 (1964).
8. E. Matijević, Acc. Chem. Res. 14, 22 (1981).
9. E. Matijević, Progr. Colloid Polym. Sci. 61, 24 (1976).
10. R. Hogg, T. W. Healy and D. W. Fuerstenau, Trans. Faraday Soc. 62, 1638 (1966).
11. B. V. Derjaguin, Disc. Faraday Soc. 18, 85 (1954).
12. B. V. Derjaguin, Kolloid Z. 69, 155 (1934).
13. J. K. Marshall and J. A. Kitchener, J. Colloid Interface Sci. 22, 342 (1966).
14. M. T. Boughey, R. M. Duckworth, A. Lips and A. L. Smith, J. Chem. Soc. Faraday Trans I 74, 2200 (1978).
15. H. Sasaki, E. Matijević and E. Barouch, J. Colloid Interface Sci. 76, 319 (1980).
16. R. J. Kuo and E. Matijević, J. Colloid Interface Sci. 78, 407 (1980).
17. E. Matijević, R. J. Kuo and H. Kolny, J. Colloid Interface Sci. 80, 94 (1981).
18. F. K. Hansen and E. Matijević, J. Chem. Soc. Faraday Trans. I 76, 1240 (1980).
19. E. Barouch, E. Matijevic, T. A. Ring and J. M. Finlan, J. Colloid Interface Sci. 67, 1 (1978); 70,29 (1979).
20. A. Bleier and E. Matijević, J. Chem. Soc. Faraday Trans. I 74, 1346 (1978).
21. E. Barouch, J. D. Nelligan and E. Matijević, J. Colloid Interface Sci. (in press).
22. R. J. Kuo and E. Matijević, J. Chem. Soc. Faraday Trans. I 75, 2014 (1979).
23. N. Kallay and E. Matijević, J. Colloid Interface Sci. (in press).
24. E. A. Cassell, K. M. Kaufman and E. Matijević, Water Res. 9, 1017 (1975).
25. M. Koishi and E. Matijević, J. Colloid Interface Sci. 79, 486 (1981).
26. H. Nakayama, E. Matijević, and K. Shinoda, J. Colloid Interface Sci. 61, 590 (1977).
27. H. Nakayama, K. Itoh, K. Shinoda and E. Matijević, Bull. Chem. Soc. Japan 53, 2493 (1980).
28. E. A. Cassell, A. J. Rubin, H. B. Lafever and E. Matijević, Water Waste Eng. 6, C7 (1969).
29. F. J. Mangravite, Jr., T. D. Buzzell, E. A. Cassell, E. Matijević and G. B. Saxton, J. Amer. Water Works Assoc. 67, 88 (1975).
30. E. A. Cassell, E. Matijević, F. J. Mangravite, Jr., T. M. Buzzell and S. B. Blabac, AIChE J. 17, 1486 (1971).
31. J. B. Melville and E. Matijević, J. Colloid Interface Sci. 57, 94 (1976).
32. F. J. Mangravite, Jr., E. A. Cassell and E. Matijević, J. Colloid Interface Sci. 39, 357 (1972).